

pubs.acs.org/Macromolecules Article

# Adding Polypeptides to the Toolbox for Redox-Switchable Polymerization and Copolymerization Catalysis

Matthew S. Thompson, Stephanie A. Johnson, Stella A. Gonsales, Gretchen M. Brown, Samantha L. Kristufek, and Jeffery A. Byers\*



**Cite This:** *Macromolecules* 2023, 56, 3024–3035



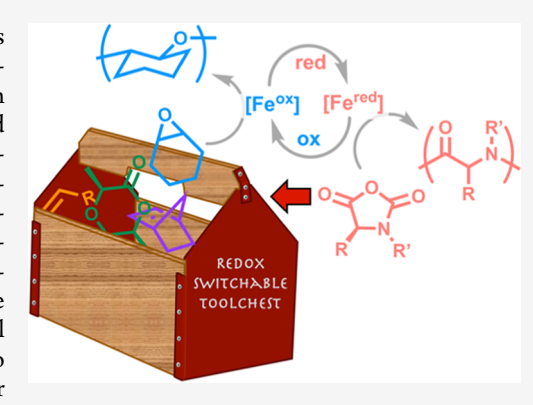
**ACCESS** I

III Metrics & More

Article Recommendations

s Supporting Information

**ABSTRACT:** Bis(imino)pyridine (BIP) iron alkoxide complexes act as catalysts to efficiently polymerize *N*-carboxyanhydrides (NCAs), including *γ*-benzyl-L-glutamate NCA (BLG-NCA) and sarcosine NCA (Sar-NCA), at room temperature. Reaction rates were greatly enhanced with the addition of mild Lewis acids, such as  $[CoCp_2][BAr^{F24}]$ , which work cooperatively with the iron-based catalysts to facilitate NCA polymerization. The reactivity of ( $^{2,6Me}BIP$ )-FeOCH<sub>2</sub>C(CH<sub>3</sub>)<sub>3</sub> with Sar-NCA was combined with its known reactivity for ε-caprolactone polymerization to form diblock and triblock copoly(ester-*b*-peptides) through sequential addition of lactone and NCA monomers. Redox-switchable polymerization reactions were developed by iteratively exposing the catalyst to redox reagents and Sar-NCA or cyclohexene oxide. The orthogonal reactivity demonstrated by the catalyst in its oxidized and reduced states led to the synthesis of diblock and triblock copoly(ether-*b*-peptides). Polyether



segments were synthesized with the catalyst in its oxidized state, while the polyamide segments were synthesized with the catalyst in its reduced state. Both copolymerization reactions developed here are rare examples where NCA polymerization reactions can be combined with other ring-opening polymerization reactions to make copolymers containing polypeptides and other functional monomers.

#### INTRODUCTION

Polyamides are a versatile class of thermoplastics whose high thermal stability and tunable mechanical properties are appropriate for a wide variety of applications, including textiles, fibers, and as engineering materials. While industrial polyamides are most commonly synthesized using step-growth polymerization reactions from diamines and diacids, 1,3 synthetic polypeptides derived from amino acids are usually obtained from the ring-opening polymerization of N-carboxyanhydrides (NCAs). The chain-growth polymerization of NCAs is most commonly achieved using primary amine initiators in highly polar solvents like dimethylformamide.5,6 This method typically produces polypeptides with good control over molecular weight, but they often require multiple days to reach completion under ambient conditions. There has been extensive progress to increase efficiency for amine-initiated reactions, which includes removing CO<sub>2</sub>,<sup>7–9</sup> using polyamine initiators, <sup>10–12</sup> using halogenated solvents, <sup>13</sup> using biphasic systems with poly(ethylene)glycol amine initiators, 14,15 using carboxylate initiators, 16 and using Nheterocyclic carbenes as catalysts. 17,18 Transition metal-based catalysts derived from low-valent metals, 19 early transition metals,<sup>20</sup> and nickel<sup>21</sup> with diverse ligand frameworks are also known and have been used to efficiently produce various polypeptides.<sup>19</sup> Despite the number of initiators and catalysts

known to polymerize NCAs, copolymers that incorporate NCA monomers with other monomers (e.g., lactones, cyclic carbonates, epoxides, etc.) are uncommon. <sup>22,23</sup> These copolymers are attractive because they diversify the mechanical properties of the polyamides, <sup>24–26</sup> have improved biocompatibility and degradability, <sup>27,28</sup> and/or phase-separate to make polymer micelles that are useful in drug delivery applications. <sup>4,29–31</sup>

Most reported syntheses of block copolymers that contain polyamides are synthesized from amine-terminated, macromolecular initiators (Scheme 1A). <sup>26,32-34</sup> These macromolecular initiators are obtained through postpolymerization functionalization or deprotection sequences, which can be difficult to carry out quantitatively and require multistep synthetic sequences. With respect to one-pot copolymer syntheses, Pahovnik and co-workers reported a general method that relies on the single insertion of an NCA monomer to polyester or polycarbonate macroinitiators under acidic

Received: November 22, 2022 Revised: March 7, 2023 Published: April 7, 2023





Scheme 1. Previous Methods to Produce Copolymers of Polyamides and Other Polymers: (a) End Group Deprotection of a Macroinitiator; (b) Sequential Addition of Strong Acids and Bases; Methods Reported in This Work Using Iron-Based Catalysts: (c) Sequential Addition of Monomers; and (d) Redox-Switchable Copolymerization

#### Previous work

Scheme 2. Iron Bis(iminopyridine) Alkoxide Complexes Used in Redox-Switchable Copolymerizations of (Left) Lactide and Cyclohexene Oxide (CHO) and (Right) NCAs and CHO

conditions followed by careful addition of a base to initiate NCA polymerization (Scheme 1B). While this method provided access to poly(ester-b-amide) and poly(carbonate-b-amide) block copolymers, the multistage reactions took several days to complete. The Guo group demonstrated that tin octanoate can be used for the copolymerization of the N-substituted sarcosine NCAs and  $\varepsilon$ -caprolactone ( $\varepsilon$ -CL). While polymerization of Sar-NCA is rapid at room temperature under active nitrogen flow, the subsequent polymerization of the lactone requires elevated temperatures (110 °C)

to produce the desired poly(amide-*b*-ester). Thomas and coworkers were able to synthesize A–B–A′ triblock copolymers of an NCA and *rac*-lactide through the sequential addition of monomers to an aluminum salen chloride catalyst and a bis(triphenyl)iminium chloride cocatalyst.<sup>36</sup> Their method does require a preactivation step in the epoxide solvent to generate an alkoxide initiator in situ. Herein, we describe a complementary approach that uses an iron-based polymerization catalyst to carry out the efficient polymerization of NCAs and can produce block copolymers either through

Table 1. Polymerization of BLG-NCA by Various Iron Bis(iminopyridine) Alkoxide Complexes with and without Additives<sup>a</sup>

entry	[Fe]	additive	time (h)	conv. (%) <sup>b</sup>	$M_{\rm n}({\rm theo})^c \ ({\rm kDa})$	$M_{\rm n}(\exp)^d$ (kDa)	$M_{\rm w}/M_{\rm n}^{}$
1	1	none	24	36	3.9	3.7	1.15
2	3	none	24	38	8.3	4.6	1.18
3	2	none	48	10	1.0	22.4	2.36
4	4	none	48	0	N/A	N/A	N/A
5	N/A	FcBAr <sup>F24</sup>	48	0	N/A	N/A	N/A
6	N/A	Fc	48	0	N/A	N/A	N/A
7	N/A	$CoCp_2$	0.17	>99	21.9	73.8	2.38
8	N/A	$[CoCp_2][BAr^{F24}]$	48	0	N/A	N/A	N/A
9	3	Fc	24	37	8.1	5.3	1.32
10	3	$[CoCp_2][BAr^{F24}]$	8	99	21.5	13.0	1.32
11	3	$[CoCp_2][PF_6]$	8	92	20.1	14.1	1.30
12	3	$[CoCp_2^*][BAr^{F24}]$	24	26	5.7	1.7	1.70
13	3	$B(C_6F_5)_3$	24	0	N/A	N/A	N/A
14	3	$Zn(^{4,4t\text{-bu}}bpy)Cl_2$	24	70	15.3	13.1	1.27

<sup>&</sup>lt;sup>a</sup>Reactions were carried out at room temperature in THF using 1:1:100 catalyst/additive/monomers at [0.35 M] relative to the monomer. <sup>b</sup>Conversion determined by <sup>1</sup>H NMR. <sup>c</sup>Theoretical molecular weight  $M_n(\text{theo}) = \text{conv.*}(MW_{BLG-NCA} - MW_{CO_2})*([\text{monomer}]/[\text{initiator}])$ . <sup>d</sup>Determined by size-exclusion chromatography relative to polystyrene standards using an RI detector.

sequential addition of monomers (for polyester copolymers, Scheme 1C) or through redox-switchable polymerization reactions (for polyether copolymers, Scheme 1D). The catalysis is efficient and proceeds in one pot, providing convenient access to useful polypeptide copolymers that incorporate other functional monomers.

#### ■ RESULTS AND DISCUSSION

An emerging area in synthetic polymer chemistry is switchable polymerization reactions, 37,38 which rely on the application of an external stimulus to alter the rate or selectivity of a polymerization reaction in situ so as to control polymer composition and/or architecture. Switchable polymerization reactions have been used to efficiently produce block copolymers, 37,39-42 to control branching, 43,44 and to trigger crosslinking reactions. 41,45,46 Several external stimuli have been used in switchable polymerization reactions including gas pressure, 47,48 pH, 46 and light, 45,49,50 but particularly prevalent has been the use of redox reactions that alter the reactivity of redox-active polymerization catalysts. 39,51-56 Over the past few years, we have been investigating a family of iron-based catalysts that have redox-switchable characteristics for the polymerization of lactide and epoxides (left, Scheme 2).41,54,57,58 We have leveraged this reactivity to control the monomer sequence in block copolymers starting from mixtures of monomers, 54,57 to develop redox-triggered crosslinking reactions, 41 and for patterning in surface-initiated polymerization reactions. 58,59 Recently, we have also developed an electrochemical method that can be used instead of chemical redox reagents to control the polymerization reactions.<sup>54</sup> Although redox-switchable polymerization catalysts are known for alkenes, 55,56 lactones including lactide, 39,51,52,60 and epoxides, 42,54,57 they have not been developed for the polymerization of NCAs. We anticipated that the versatility of the bis(imino)pyridine (BIP) iron complexes for ringopening polymerization reactions could be exploited to create a redox-switchable catalytic system that would also be amenable for the production of block copolymers containing polyamides (right, Scheme 2).

We have previously reported the synthesis of iron BIP complexes 1-3, which led to a family of complexes that differed by charge, formal oxidation state, and coordination

number (Scheme 2).<sup>51,61</sup> Access to a cationic iron complex 4 would provide a second possible catalyst combination (i.e., 3 and 4) that could be used for redox switching. We expected that this combination would demonstrate different reactivity for NCA polymerization compared to the original redox-switchable catalytic system (i.e., 1 and 2). Fortunately, complex 4 could be easily accessed by oxidizing neutral iron complex 3 with ferrocenium tetrakis(3,5-bis(trifluoromethyl)-phenyl)borate (FcBAr<sup>F24</sup>), which proceeded cleanly as evidenced by <sup>1</sup>H, <sup>11</sup>B, and <sup>19</sup>F NMR spectroscopy (see the Supporting Information).

To understand what catalyst features are best for NCA polymerization, the activities of 1–4 were evaluated for the polymerization of  $\gamma$ -benzyl-L-glutamate N-carboxyanhydride (BLG-NCA) (entries 1–4, Table 1). These studies revealed that neutral, iron complexes 1 and 3 were active for the polymerization of BLG-NCA, reaching a conversion of 36 and 38%, respectively, after 24 h (entries 1 and 2, Table 1). The polymers obtained from these reactions had low dispersities and molecular weights that were generally lower than predicted. However, due to instrument limitations, molecular weights were determined by size-exclusion chromatography relative to polystyrene standards, which likely contributes to the difference between theoretical and experimental molecular weights (Table S2).

Full conversion of the monomer was not observed under these conditions (Table S2), which we hypothesized is due to product inhibition resulting from coordination of the polymer amide group to the catalyst. In order to get a better sense of the relative activities of 1 and 3 without complications from product inhibition, each catalyst precursor was evaluated by monitoring reactions at lower conversions (Table S2). These experiments revealed that complex 1 and complex 3 have very similar reactivity with 3 being slightly more active than 1. This trend is likely a consequence of 3 containing the more electron-rich metal center compared to 1 (formally Fe(I) vs Fe(II), respectively), which is consistent with NCAs being more commonly polymerized with base initiators<sup>4,5</sup> rather than acid catalysts. 35,63 In contrast to 1 and 3, cationic iron complexes 2 and 4 were much less active for BLG-NCA polymerization. Reactions catalyzed by 2 were slow, leading to only 10% conversion after 48 h with a broad molecular weight

distribution and significant tailing toward higher molecular weights (entry 3, Table 1), while complex 4 did not react with BLG-NCA even after extended reaction times (entry 4, Table 1). Thus, the overall reactivity of the family of complexes toward NCA polymerization is  $3 > 1 > 2 \gg 4$ .

The orthogonal reactivity of 3 and 4 toward the polymerization of BLG-NCA made it suitable for a potential redox-switchable polymerization system. To this end, redox switching through the iterative addition of chemical redox reagents was pursued (Figure 1). Addition of FcBAr<sup>F24</sup> to BLG-NCA

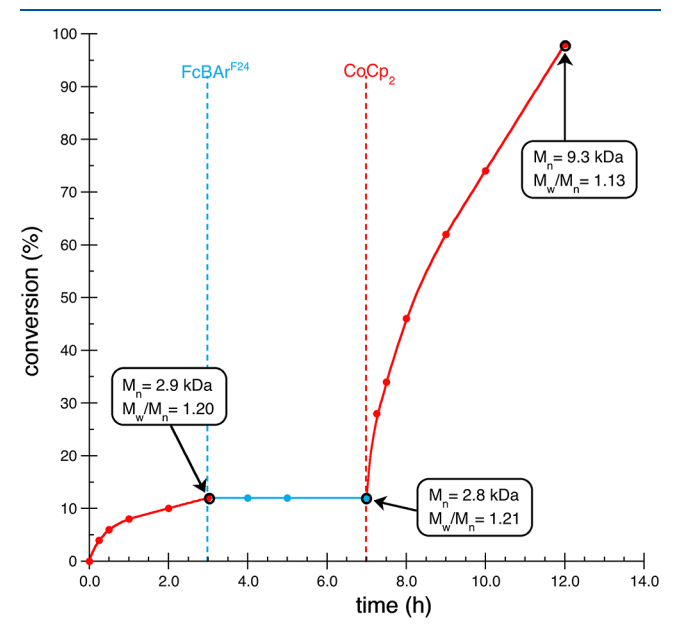


**Figure 1.** Redox-switchable polymerization of BLG-NCA by complex 3 in THF at room temperature. Oxidation and reduction of the catalyst are represented with dotted lines and are enacted with the addition of FcBAr<sup>F24</sup> and CoCp<sub>2</sub>, respectively. The red and blue data points indicate when the catalyst is in the reduced and oxidized oxidation states, respectively. Number-averaged molecular weights  $(M_{\rm n})$  and molecular weight distributions  $(M_{\rm w}/M_{\rm n})$  for the indicated data points were determined by GPC relative to polystyrene standards.

polymerization reactions catalyzed by 3 led to an immediate color change, which was indicative of catalyst oxidation. Concurrent with catalyst oxidation, no further BLG-NCA polymerization was observed as expected. Furthermore, no change in molecular weight or molecular weight distribution was observed even after stirring for an additional 4 h. Addition of cobaltocene (CoCp2) reduced the catalyst and led to consumption of the BLG-NCA monomer, which was more rapid than observed initially. Moreover, the catalyst was no longer limited to low conversion and instead reached an ultimate conversion of 99% 4 h after adding CoCp2 (Figure 1). Despite the significant increase in the reaction rate, molecular weight distributions remained narrow  $(M_{\rm w}/M_{\rm n}=1.13)$ , suggesting a single active catalyst.

The dramatic increase in activity observed after the catalyst underwent oxidation and reduction in redox-switchable polymerization reactions warranted further investigation. The reactivity of the redox reagents (i.e., FcBAr<sup>F24</sup> and CoCp<sub>2</sub>) and the byproducts from the redox reactions (i.e., Fc and [CoCp<sub>2</sub>][BAr<sup>F24</sup>]) revealed that only CoCp<sub>2</sub> was active for BLG-NCA polymerization in the absence of 3 (entries 5–8, Table 1). The polymerization initiated by CoCp<sub>2</sub> alone was

rapid, reaching completion in less than 10 min (entry 7, Table 1). Unlike the redox-switchable polymerization reaction, however, a significantly higher-molecular-weight polymer was obtained ( $M_{\rm n}=73.8~{\rm kg/mol}$ ), and the polymer had a broad molecular weight distribution ( $M_{\rm w}/M_{\rm n}=2.38$ ). The better molecular weight control along with the rapid color change (occurring in seconds) observed during the redox-switchable polymerization reaction led us to conclude that electron transfer from CoCp<sub>2</sub> to the catalyst was faster than direct polymerization of BLG-NCA with CoCp<sub>2</sub>. Consequently, we concluded that the iron-based catalyst is solely responsible for the redox-switchable polymerization.

In order to explain the increased reaction rate observed after catalyst reduction in the redox-switchable polymerization reaction, a mechanism was considered that involved cooperative catalysis between the reduced iron-based catalyst 3 and one or more of the chemical byproducts formed from redox switching (i.e., Fc or [CoCp<sub>2</sub>][BAr<sup>F24</sup>]). To test this hypothesis, BLG-NCA polymerization reactions were carried out in the presence of catalyst 3 and independently prepared Fc or [CoCp<sub>2</sub>][BAr<sup>F24</sup>] (entries 9 and 10, Table 1). Relative to reactions catalyzed by 3, no rate enhancement was observed when Fc was added to the reaction. In contrast, when [CoCp<sub>2</sub>][BAr<sup>F24</sup>] was added to the reaction, rate enhancement similar to the one observed in the redox-switchable polymerization reaction was observed. These results suggested that [CoCp2]+ could act as a weak Lewis acid, which may work in concert with 3 to enhance NCA polymerization rates. Exchanging the BAr<sup>F24</sup> anion with the PF<sub>6</sub> anion had minimal influence on the polymerization rate (entry 11, Table 1), suggesting that the anion has little effect on the reaction. In contrast, when the sterically more encumbered and more electron-rich decamethylcobaltocenium tetrakis (3,5-bis-(trifluoromethyl)phenyl)borate ([CoCp<sub>2</sub>\*][BAr<sup>F24</sup>]) was used as an additive, no noticeable rate enhancement was observed (entry 12, Table 1). This outcome is consistent with the additive serving as a Lewis acid since the more electronrich and bulkier [CoCp<sub>2</sub>\*]<sup>+</sup> is less Lewis acidic than [CoCp<sub>2</sub>]<sup>+</sup>.

To further verify the role of  $[CoCp_2]^+$  as a Lewis acid, a number of Lewis acidic additives were investigated (Tables 1 and S2). The strong Lewis acid  $B(C_6F_5)_3$  completely shut down the reaction, a likely consequence of the borane reacting irreversibly and unproductively with 3 (entry 13, Table 1). Similar trends occurred with other strong Lewis acidic (entries 22–24, Table S2). In contrast, mildly Lewis acidic additives, such as  $(4,4'\text{-di-}tert\text{-butyl-}2,2'\text{-bipyridine})\text{ZnCl}_2$ , led to enhanced reaction rates while maintaining good control over molecular weight (entry 14, Table 1). These results suggested that mild Lewis acids were suitable cocatalysts for the polymerization of NCAs with 3. Since  $[CoCp_2][BAr^{F24}]$  was slightly more effective as a Lewis acidic additive, it was chosen for all subsequent NCA polymerization reactions.

We next explored how [CoCp<sub>2</sub>][BAr<sup>F24</sup>] affected the redox-switchable polymerization of BLG-NCA (Figure 2). When a reaction starting with a mixture of BLG-NCA and [CoCp<sub>2</sub>]-[BAr<sup>F24</sup>] was exposed to the iron complex 3, we observed a rapid polymerization before oxidation and after reduction, which is consistent with the rate enhancements observed previously in the presence of the cobaltocenium cocatalyst (Figure 1). Notably, additional equivalents of [CoCp<sub>2</sub>]-[BAr<sup>F24</sup>] formed from the redox switching process did not influence the polymerization rates significantly. While BLG-NCA polymerization reactions catalyzed by 3 demonstrated

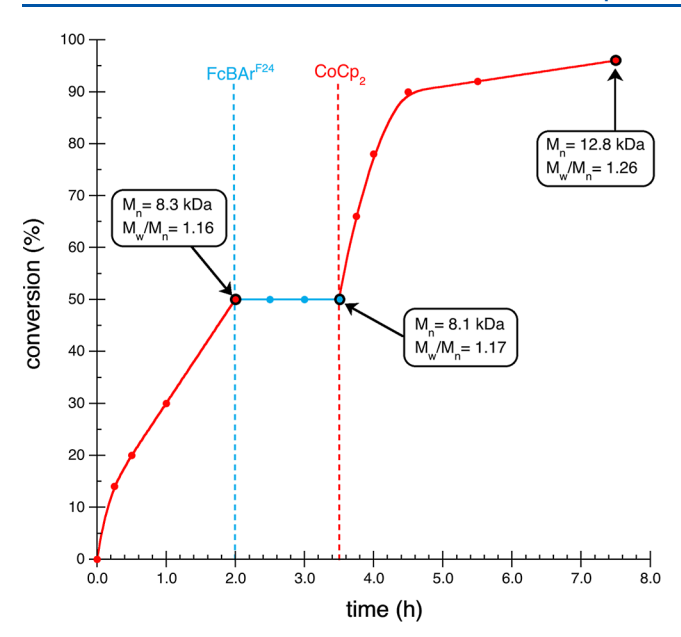


**Figure 2.** Redox-switchable polymerization of BLG-NCA by complex  $3/[\mathrm{Cp_2BAr^{F24}}]$  in THF at room temperature. Oxidation and reduction of the catalyst are represented with dotted lines and are enacted with the addition of FcBAr<sup>F24</sup> and CoCp<sub>2</sub>, respectively. The red and blue data points indicate when the catalyst is in the reduced and oxidized oxidation states, respectively.  $M_{\rm n}$  and  $M_{\rm w}/M_{\rm n}$  for the indicated data points were determined by GPC.

narrow molecular weight distributions  $(M_w/M_n < 1.35)$ , molecular weights remained lower than expected and did not increase significantly with conversion. While the low molecular weights could be due to the fact that molecular weights were determined relative to polystyrene standards, the fact that molecular weights did not change over the course of the reaction was troubling. End-group analysis using <sup>1</sup>H NMR spectroscopy (Figure S6) and MALDI-TOF mass spectrometry (Figure S7) of poly(γ-benzyl-L-glutamate) obtained with 3 as the catalyst revealed that the alkoxide initiator was not incorporated as an end group. This observation suggested that the BLG-NCA polymerization reactions are not initiated by the alkoxide initiator but instead are likely initiated by the first N-H deprotonation of BLG-NCA by 3. Free neopentanol observed by <sup>1</sup>H NMR spectroscopy in the reaction solution supported this notion.

It is known that exceptionally basic additives will initiate NCA polymerization by deprotonating NCA monomers,  $^{4,64,65}$  but these polymerization reactions produce a polymer with high molecular weights and/or broader molecular weight distributions (i.e.,  $M_{\rm w}/M_{\rm n}=2-5$ ) compared to what was observed when 3 was used as the catalyst. We also tested the bulky base, KO<sup>6</sup>Bu, as an initiator for BLG-NCA polymerization and observed rapid polymerization, reaching >99% conversion in 10 min, and the resulting polymer possessed a broad dispersity ( $M_{\rm w}/M_{\rm n}=3.31$ ) (Table S2). Therefore, instead of an anionic polymerization mechanism initiated by 3, we favor a coordination-insertion mechanism initiated by

Scheme 3. Proposed Coordination-Insertion Mechanism for BLG-NCA (R = CH<sub>2</sub>CH<sub>2</sub>CO<sub>2</sub>Bn); (a) and Sar-NCA (b) Polymerization Catalyzed by 3 and Cocatalyzed by a Lewis Acid Cocatalyst (LA)<sup>a</sup>

<sup>a</sup>The Lewis acidic cocatalyst could serve two functions: to activate NCA for insertion and to prevent product inhibition. The propagation mechanism is more complex than shown as we demonstrate in an analogous work in which we studied the ring-opening polymerization by 3 computationally.<sup>69</sup>

Table 2. Polymerization of Sar-NCA by Iron Bis(iminopyridine) Complexes 3 and 4<sup>a</sup>

entry	catalyst	[Fe] (x mol %)	conversion (%) <sup>b</sup>	$M_{\rm n}({\rm theo})~({\rm kDa})^c$	$M_{\rm n}({\rm exp})~({\rm kDa})^d$	$M_{\rm w}/M_{\rm n}^{}$
1	3	1	70	5.0	5.0	1.15
2 <sup>e</sup>	3	1	71	5.0	5.8	1.06
$3^f$	3	1	70	5.0	3.7	1.48
4	3	2	65	2.5	3.0	1.35
5	3	0.5	67	9.5	9.6	1.05
6	3	0.025	71	19.9	20.3	1.03
$7^g$	3	1	>99	7.1	7.1	1.06
8	4	1	0	N/A	N/A	N/A

"Reactions were carried out for 10 min in THF using complex 3 at [0.35 M] relative to monomer. Conversion was determined by H NMR and the mass of the precipitated polymer. Theoretical molecular weight  $M_n(\text{theo}) = \text{conv.*}(MW_{\text{Sar-NCA}} - MW_{\text{CO}_2})*100$ . Determined by GPC vs polystyrene standards. Reaction ran for 4 h. Reaction ran for 24 h.  $g[\text{CoCp}_2][\text{FcBAr}^{\text{F24}}]$  (1 mol %) was also added to the reaction.

deprotonation of the BLG-NCA monomer (Scheme 3A).<sup>66</sup> Deprotonation of BLG-NCA by 3 leads to complex 5, which can then insert into a second BLG-NCA monomer to produce iron carbamate complex 6. Decarboxylation produces iron amide complex 7, which can propagate polymerization by inserting into BLG-NCA to regenerate complex 6.

The role of the Lewis acid additive can also be explained if a coordination-insertion mechanism were operative (Scheme 3). The Lewis acid may bind to the NCA to activate it for insertion from the basic iron alkoxide 3 or amide intermediates 5 or 7. Another likely role for the Lewis acid cocatalyst is to prevent product inhibition. After insertion of an NCA monomer and decarboxylation to form intermediate 7, the amide carbonyl from the newly formed peptide is ideally situated to form a five-membered ring chelate with iron to form complex 8. If formed, 8 would inhibit polymerization by preventing the next NCA monomer from binding to the catalyst. However, in the presence of a Lewis acidic cocatalyst, the amide carbonyl can interact with the Lewis acid instead of the iron center, thereby freeing up the metal for subsequent NCA enchainment. Extensive mechanistic studies into the origin of the cocatalyst effect are beyond the scope of this paper, but we did carry out two additional experiments that provided some insight. First, we analyzed a mixture of [CoCp<sub>2</sub>][BAr<sup>F24</sup>] and Sar-NCA by <sup>1</sup>H NMR to see if a Lewis acid/base pair could be identified as unique resonances in the NMR. However, this experiment revealed no new resonances in the NMR spectrum, which either suggested the absence of a Lewis acid/base pair or rapid equilibrium that occurs faster than the NMR timescale. Second, mixing dimethyl amine in THF with [CoCp2][BArF24] resulted in significant retardation in polymerization initiated by the amine rather than enhanced rates observed when [CoCp<sub>2</sub>][BAr<sup>F24</sup>] was combined with 3. These experiments further demonstrated that the polymerization mechanism involving the iron-based catalyst 3 differs significantly compared to amine-initiated polymerization reactions.

To test whether deprotonation of BLG-NCA is responsible for the behavior described above, 3 was evaluated as a catalyst for sarcosine N-carboxyanhydride (Sar-NCA) polymerization (Table 2). Unlike BLG-NCA, Sar-NCA does not contain an acidic N–H proton, which would preclude formation of complex 5 being formed as well as the chain transfer mechanism pathway proposed in Scheme 3. In the absence of  $[CoCp_2][BAr^{F24}]$ , complex 3 was very active in the polymerization of Sar-NCA. The reaction reached 70% conversion in only 10 min at room temperature; further conversion was not seen at extended reaction times (entry 1,

Table 2). Little change was seen when the reaction continued to run for 4 h, but prolonged stirring for 24 h led to molecular weight decrease and dispersity increase (entries 2 and 3, Table 2). The lower molecular weight and increased dispersity are likely due to backbiting reactions, which may prevail at high conversions. The polymerization once again displayed narrow molecular weight distributions, and molecular weights were close to the theoretical molecular weights. Moreover, molecular weights changed with catalyst loading, which is typical for polymerizations that proceed with good molecular weight control (entries 4-6, Table 2). Unlike polymer obtained from BLG-NCA polymerizations (Figures S6 and S7), end-group analysis of the polymer obtained from sar-NCA by <sup>1</sup>H NMR (Figure S12) and MALDI (Figure S13) revealed the presence of an ester end group. These observations are consistent with the mechanistic hypothesis shown in Scheme 3b. Without the ability to deprotonate the NCA monomer, initiation of Sar-NCA occurs from insertion of the alkoxide into the NCA monomer. We also noted that a small amount of cyclic oligomers were also detected in the MALDI spectrum and as low molecular weight tails in the GPC spectrum. These oligomers indicate that some backbiting occurs during Sar-NCA polymerization which is currently a limitation of this catalyst.

Similarly to BLG-NCA polymerization reactions, Sar-NCA polymerization reactions catalyzed by 3 could reach full conversion without loss in molecular weight control when  $[\text{CoCp}_2][\text{BAr}^{\text{F24}}]$  was added to the reaction (entry 7, Table 2). Moreover, the oxidized complex 4 was completely inactive for Sar-NCA polymerization (entry 8, Table 2). Overall, these results demonstrated that 3 was an excellent catalyst for N-substituted NCA polymerization reactions, especially in the presence of the Lewis acidic additive  $[\text{CoCp}_2][\text{BAr}^{\text{F24}}]$ , and the catalyst also demonstrated great potential to be used in a redox-switchable system (vide infra).

Although our above mechanisms account for the role of the alkoxide initiator and the Lewis acid cocatalyst, they do not account for the significant differences in the reaction rate between the two monomers. While sterics may play a role in the slower polymerization rate of BLG-NCA, we would also like to recognize that poly(BLG) is known to form  $\alpha$ -helices in low-dielectric solvents, while poly(Sar) adopts a random coil in a number of solvents which may also be occurring in THF. The secondary structure of the growing chain may influence the accessibility of the iron catalyst to additional monomers. Further investigation of this phenomenon and its influence on the reaction rate is beyond the scope of this paper.

Scheme 4. (A) Diblock Copolymerization of  $\varepsilon$ -CL and Then Sar-NCA by  $3/[CoCp_2][BAr^{F24}]$  through Sequential Addition of Monomers; (B) Telechelic, Triblock Copolymerization of  $\varepsilon$ -CL and Then Sar-NCA by  $9/[CoCp_2][BAr^{F24}]$  through Sequential Addition of Monomers

a

(200 equiv.)

NpO

THF, rt
10 min

$$M_n(\text{GPC}) = 19.7 \text{ kDa}$$
 $M_n(\text{NMR}) = 19.6 \text{ kDa}$ 
 $M_n(\text{MMR}) = 19.6 \text{ kDa}$ 
 $M_n(\text{MMR}) = 10.2$ 

THF, rt, 10 min

 $M_n(\text{MMR}) = 10.2$ 
 $M_n(\text{MMR}) = 10.2$ 
 $M_n(\text{MMR}) = 10.2$ 
 $M_n(\text{MMR}) = 10.2$ 

THF, rt, 10 min

 $M_n(\text{MMR}) = 10.2$ 
 $M_n(\text{MMR}) = 1$ 

With the combination of 3 and [CoCp<sub>2</sub>][BAr<sup>F24</sup>] established as a good catalyst for the polymerization of Sar-NCA that incorporated the alkoxide initiator as an end group, we decided to leverage the exceptional activity of 3 for lactone polymerization<sup>61,69</sup> to form copolymers between Sar-NCA<sup>70</sup> and  $\varepsilon$ -CL (Scheme 4A). As expected, exposing 3 to  $\varepsilon$ -CL followed by [CoCp<sub>2</sub>][BAr<sup>F24</sup>] and Sar-NCA led to the production of copoly(ester-b-amide) block copolymers (Scheme 4A), which was indicated by <sup>1</sup>H NMR spectroscopy (Figure S19). The polymer obtained was of moderately high molecular weight and narrow molecular weight distribution ( $M_n = 31.2 \text{ kDa}$ ,  $M_{\rm w}/M_{\rm n}$  = 1.08) (Scheme 4A), and the block copolymer microstructure was verified using DOSY spectroscopy (Figure S20). Encouraged by these results and motivated by the possibility of forming a thermoplastic elastomer with the synthesis of an A–B–A poly(amide-b-ester-b-amide) triblock copolymer, the opposite order of monomer addition was explored next. Unfortunately, the polymer produced from Sar-NCA polymerization catalyzed by  $3/[CoCp_2][BAr^{F24}]$  ( $M_n =$ 6.9 kDa,  $M_{\rm w}/M_{\rm n}$  = 1.04) was not capable of initiating  $\varepsilon$ -CL polymerization, even with temperatures up to 60 °C and prolonged reaction times. The inactivity toward  $\varepsilon$ -CL was particularly surprising considering the exceptional activity that 3 had for the polymerization of  $\varepsilon$ -CL. <sup>61,69</sup> We hypothesize that the decreased reactivity of  $\varepsilon\text{-CL}$  after Sar-NCA polymerization is likely due to the ability of the polyamide carbonyls to chelate to the iron catalyst (e.g., intermediate 8, Scheme 3), which can be sufficiently overcome with the addition of [CoCp<sub>2</sub>][BAr<sup>F24</sup>] for NCA monomers but not for the less nucleophilic  $\varepsilon$ -CL monomer.

Despite this limitation, A-B-A poly(amide-b-ester-b-amide) triblock copolymers were accessible using a telechelic polymerization approach (Scheme 4B). The addition of the

diol initiator 1,4-benzenedimethanol to BIP iron alkyl precursor 9 generated an alkoxide catalyst in situ, which was suitable to initiate  $\varepsilon$ -CL polymerization. The molecular weight of the polyester produced was close to the theoretical amount at >99% conversion as determined by GPC and NMR  $(M_n(\exp,GPC) = 58.8 \text{ kDa}; M_n(\exp,NMR) = 50.2 \text{ kDa};$  $M_{\rm n}({\rm theor}) = 45.8~{\rm kDa}$ ), and the molecular weight distribution was narrow  $(M_w/M_n = 1.17)$  (Scheme 4B). Addition of [CoCp<sub>2</sub>][BAr<sup>F24</sup>] and Sar-NCA led to efficient conversion of the NCA monomer and production of the A-B-A poly-(amide-*b*-ester-*b*-amide) triblock copolymer ( $M_n(GPC) = 75.9$ kDa,  $M_w/M_n = 1.16$ ,  $M_n(NMR) = 73.1 kDa$ ) (Scheme 4B), which was supported by <sup>1</sup>H NMR and DOSY spectroscopy (Figures S22 and S23). Monomodal molecular weight distributions of the resulting copolymers were observed by GPC along with a clear increase in molecular weight, supporting chain elongation at all molecular weights (Figure 3).

We next pursued the synthesis of block copolymers containing polyamides and polyethers. In order to synthesize such copolymers, a redox-switchable polymerization strategy was explored. Previously, the cationic, formally iron(III) complex 2 was shown to be active for epoxide polymerization, <sup>57</sup> which neutral, formally iron(II) complex 1 is inactive toward. <sup>61</sup> The complementary reactivity observed between 1 and 2 inspired the development of a redox-switchable polymerization reaction between lactide and epoxides that led to the production of block copolymers either from sequential addition of monomers or from a pool of both monomers. <sup>57</sup> Considering that 4 was also a cationic iron complex, it was expected that it would exhibit similar reactivity as complex 2 for epoxide polymerization. Validation of this expectation would then make the redox-switchable copoly-

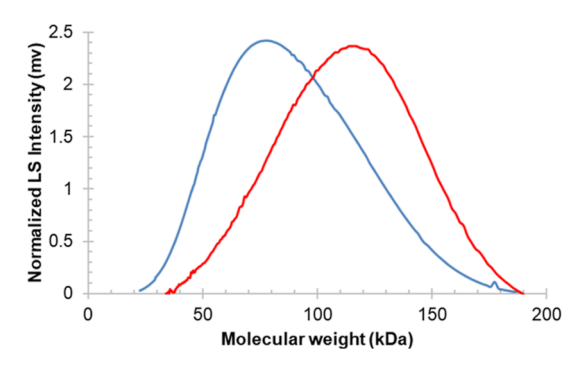


**Figure 3.** GPC chromatogram from the telechelic copolymerization of  $\varepsilon$ -CL (blue,  $M_{\rm n}=58.8$  kDa,  $M_{\rm w}/M_{\rm n}=1.17$ ) and then Sar-NCA (red,  $M_{\rm n}=75.9$  kDa,  $M_{\rm w}/M_{\rm n}=1.16$ ).

merization of epoxides with NCAs possible by leveraging the redox-switchable activity of 3 for NCA polymerization described above.

As anticipated, catalyst 4 was very active for CHO polymerization. As was the case with 2, CHO polymerization catalyzed by 4 did not demonstrate living characteristics, producing more dispersed polymers  $(M_w/M_p = 1.60-1.79)$ (Scheme 5) but with molecular weights more in line with theoretical molecular weights (e.g.,  $M_n(\exp) = 10.0 \text{ kg/mol}$ ,  $M_{\rm p}({\rm theo}) = 9.6 \text{ kg/mol}, M_{\rm w}/M_{\rm p} = 1.73 \text{ at } 1\% \text{ catalyst loading}$ and 98% conversion). While quantitative rate measurements are beyond the scope of this study, 4 was less efficient as a catalyst for CHO polymerization when qualitatively compared to 2,57 with polymerizations reaching high conversions in hours with 4 as opposed to minutes with 2. As was the case when 2 was used as the catalyst, no further conversion was observed when CoCp<sub>2</sub> was added to the reaction. This observation is consistent with species 3 also being inactive for CHO polymerization.

Encouraged by the orthogonal reactivity of 3 and 4 toward Sar-NCA and CHO, respectively, copolymerization reactions were next attempted, wherein the chemoselectivity of the catalyst was altered through the addition of redox reagents in situ (Scheme 5). When a mixture of Sar-NCA and CHO was

exposed to 3/[CoCp<sub>2</sub>][BAr<sup>F24</sup>], a clean conversion of Sar-NCA was observed with no conversion of CHO. Addition of FcBAr<sup>F24</sup> to the reaction led to the polymerization of CHO, which was consistent with the redox switching experiments for CHO. However, precipitation of the polymer in hexanes resulted in the isolation of separate homopolymers, specifically polysarcosine in the precipitate and soluble poly(cyclohexene oxide). To test whether the polyether obtained in this reaction reflects the activity of FcBArF24 as a catalyst for epoxide polymerization, 42 sequential addition of the monomers/ reagents was explored next (Scheme 5a). The polymerization of Sar-NCA proceeded when exposed to  $3/[CoCp_2][BAr^{F24}]$ . GPC analysis of the polysarcosine revealed a monomodal molecular weight distribution, although there was some low molecular weight tailing (Figure S25), which we attribute to backbiting at low monomer concentration due to the low solubility of Sar-NCA in 2-methyltetrahydrofuran.<sup>72</sup> When FcBar<sup>F24</sup> was added to the reaction, a rapid color change occurred, consistent with the oxidation of the iron complex. CHO was then added, and full conversion to polymer was observed. Unlike the reaction initiated with both monomers initially present, the product obtained from sequential addition of monomers and redox reagents leads to a copolymer with a monomodal molecular weight distribution by GPC (Figure S25).<sup>73</sup> <sup>1</sup>H and DOSY NMR spectroscopies (Figures S26 and \$28) were also consistent with the formation of a poly(amideb-ether) block copolymer. These results suggest that the polyether product formed in the procedure starting from a mixture of monomers likely arises from the competitive reaction of CHO with FcBArF24 instead of electron transfer between FcBAr<sup>F24</sup> and the iron-based complex. To complete the evaluation of 3-[CoCp<sub>2</sub>][BAr<sup>F24</sup>]/4 as a redox-switchable polymerization system for the production of block copolymers that contain amides and ethers, the polymerization of CHO followed by Sar-NCA was pursued (Scheme 5b). As was the case with the switch between 3 and 4, sequential addition of CoCp<sub>2</sub> to a CHO polymerization catalyzed by 4 followed by Sar-NCA led to the production of a poly(ether-b-amide) block copolymer without significant production of polyether or polyamide byproducts. Formation of the block copolymer was

Scheme 5. Synthesis of Polyether-Polyamide Diblock Copolymers Using a 3/4 Catalyzed Redox-Switchable Polymerization; (a) Poly(Sar-b-CHO) and (b) Poly(CHO-b-Sar) through the Sequential Addition of Monomers

Scheme 6. Synthesis of Poly(Sar-b-CHO-b-Sar) Triblock Copolymers Using a 3/4 Catalyzed Redox-Switchable Polymerization from Mixed Monomer Solution

confirmed by <sup>1</sup>H and DOSY NMR spectroscopies (Figures S30 and S32).

Finally, an A–B–A′ poly(amide-*b*-ether-*b*-amide′) triblock copolymer was formed through sequential addition of monomers and oxidants/reductants. To synthesize this block copolymer, 3 and [CoCp<sub>2</sub>][Bar<sup>F24</sup>] were used to polymerize Sar-NCA (Scheme 6). Upon addition of FcBAr<sup>F24</sup>, the metal complex containing a poly(Sar) chain was oxidized and the addition of CHO led to formation of the diblock copolymer poly(Sar-*b*-CHO). Addition of CoCp<sub>2</sub> followed by an additional Sar-NCA resulted in the formation of the triblock copolymer poly(Sar-*b*-CHO-*b*-Sar′) (Scheme 6). Analysis of the diblock and triblock copolymers by GPC revealed uniform chain extension and monomodal molecular weight distributions (Figure 4).<sup>73</sup> The molecular weight determined by GPC

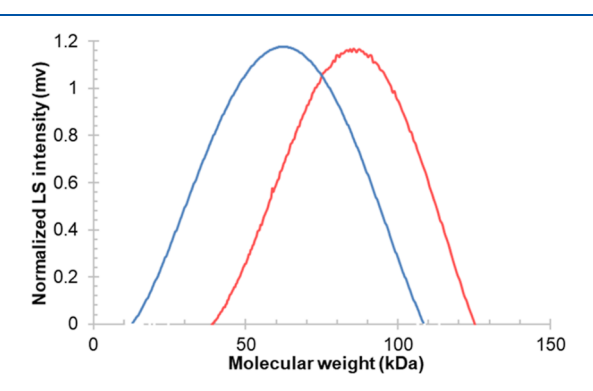


**Figure 4.** GPC chromatogram of poly(Sar-b-CHO) (blue,  $M_{\rm n}=32.2$  kDa,  $M_{\rm w}/M_{\rm n}=1.38$ , blue) and poly(Sar-b-CHO-b-Sar') (red,  $M_{\rm n}=62.2$  kDa,  $M_{\rm w}/M_{\rm n}=1.15$ ).

increases significantly after the addition of Sar-NCA (32.2–64.2 kDa), while the molecular weight determined by endgroup analysis using <sup>1</sup>H NMR increases less significantly (40.0–47.2 kDa) and better matches the theoretical molecular weight. The discrepancy in the molecular weights determined by NMR and GPC may be caused by an error in both measurements: the molecular weight of the polymer is near the threshold for assessing molecular weight by end-group analysis and the molecular weight as determined by the light-scattering detector is likely an overestimation as is common with LS

detection. The formation of the triblock copolymers was supported with <sup>1</sup>H and DOSY NMR (Figures S34 and S36).

#### CONCLUSIONS

The low-valent iron complex 3 was found to be an efficient catalyst for NCA polymerization reactions, especially when used in combination with a mild Lewis acid, such as [CoCp<sub>2</sub>][BAr<sup>F24</sup>]. Unlike most NCA polymerization reactions, the mechanism for NCA polymerization with 3 is likely a coordination-insertion mechanism that benefits from cooperative interactions with a Lewis acid cocatalyst. The similarity that this mechanism shared with the assumed mechanism for lactone polymerization catalyzed by 3 enabled these complexes to be used as catalysts for the uncommonly reported, one-pot, copolymerization reactions between NCA and lactone monomers. 22,23,35 With the appropriate order of addition and choice of initiator, diblock and triblock copolymers that incorporate Sar-NCA and  $\varepsilon$ -CL could be obtained. Moreover, complex 3 could be reversibly oxidized during the polymerizations with one electron redox reagents, which resulted in the first example of a redox-switchable polymerization of NCAs. This reactivity was combined with orthogonal reactivity of the oxidized complex 4 for CHO polymerization to produce poly(amide-b-ether) block copolymers, the composition of which could be altered through in situ addition of chemical oxidants and reductants. Future improvements to the system will include adoption of the electrochemical redox switching system we recently reported to address redox reagent incompatibility, 42 and further monomer and catalyst engineering targeting a broader set of NCA monomers for incorporation into copolymerization reactions. The success of these efforts is expected to lead to the synthesis of new polymeric materials with useful and tunable properties that would benefit a wide variety of applications from new thermoplastic materials to drug delivery devices.

#### ASSOCIATED CONTENT

#### **Solution** Supporting Information

The Supporting Information is available free of charge at https://pubs.acs.org/doi/10.1021/acs.macromol.2c02381.

Detailed experimental procedures and characterization data for polymers (PDF)

#### AUTHOR INFORMATION

#### **Corresponding Author**

Jeffery A. Byers — Eugene F. Merkert Chemistry Center, Department of Chemistry, Boston College, Chestnut Hill, Massachusetts 02467, United States; oocid.org/0000-0002-8109-674X; Email: jeffery.byers@bc.edu

#### **Authors**

- Matthew S. Thompson Eugene F. Merkert Chemistry Center, Department of Chemistry, Boston College, Chestnut Hill, Massachusetts 02467, United States; ⊚ orcid.org/ 0000-0003-1672-0486
- Stephanie A. Johnson Eugene F. Merkert Chemistry Center, Department of Chemistry, Boston College, Chestnut Hill, Massachusetts 02467, United States
- Stella A. Gonsales Eugene F. Merkert Chemistry Center, Department of Chemistry, Boston College, Chestnut Hill, Massachusetts 02467, United States
- Gretchen M. Brown Eugene F. Merkert Chemistry Center, Department of Chemistry, Boston College, Chestnut Hill, Massachusetts 02467, United States
- Samantha L. Kristufek Department of Chemistry, Massachusetts Institute of Technology (MIT), Cambridge, Massachusetts 02139, United States

Complete contact information is available at: https://pubs.acs.org/10.1021/acs.macromol.2c02381

#### Notes

The authors declare no competing financial interest.

#### ACKNOWLEDGMENTS

J.A.B. acknowledges that this material is based upon work supported by the National Science Foundation under Grant No. CHE-1955926 and the Army Research Office Grant No. W911NF-15-1-0454. S.L.K. acknowledges the fellowship from the Misrock Fund for providing resources that contributed to the research results within this paper. Marek Domin at Boston College recorded spectra for mass spectroscopy analysis. Dr. Jia Niu at Boston College provided the GPC for the characterization of polyamides.

#### REFERENCES

- (1) Marchildon, K. Polyamides Still Strong after Seventy Years. *Macromol. React. Eng.* **2011**, *5*, 22–54.
- (2) García, J. M.; García, F. C.; Serna, F.; de la Peña, J. L. High-Performance Aromatic Polyamides. *Prog. Polym. Sci.* **2010**, *35*, 623–686.
- (3) Nylon 6 & 66 Market Analysis By Product (Nylon 6, Nylon 66) By Application (Automotive, Electrical & Electronic, Engineering Plastic, Textiles, Others), By Region, And Segment Forecasts, 2018—2025, 2017. https://www.grandviewresearch.com/industry-analysis/nylon-6-6-market (accessed 4/4/2023).
- (4) Cheng, J.; Deming, T. J. Synthesis of Polypeptides by Ring-Opening Polymerization of Alpha-Amino Acid N-Carboxyanhydrides. *Top. Curr. Chem.* **2012**, *310*, 1.
- (5) González-Henríquez, C. M.; Sarabia-Vallejos, M. A.; Rodríguez-Hernández, J. Strategies to Fabricate Polypeptide-Based Structures via Ring-Opening Polymerization of N-Carboxyanhydrides. *Polymers* **2017**, *9*, 551.
- (6) Rasines Mazo, A.; Allison-Logan, S.; Karimi, F.; Chan, N. J. A.; Qiu, W.; Duan, W.; O'Brien-Simpson, N. M.; Qiao, G. G.; Neil, M.; Qiao, G. G. Ring opening polymerization of  $\alpha$ -amino acids: advances in synthesis, architecture and applications of polypeptides and their hybrids. *Chem. Soc. Rev.* **2020**, *49*, 4737–4834.

- (7) Habraken, G. J. M.; Wilsens, K. H. R. M.; Koning, C. E.; Heise, A. Optimization of N-Carboxyanhydride (NCA) Polymerization by Variation of Reaction Temperature and Pressure. *Polym. Chem.* **2011**, 2, 1322–1330.
- (8) Zou, J.; Fan, J.; He, X.; Zhang, S.; Wang, H.; Wooley, K. L. A Facile Glovebox-Free Strategy to Significantly Accelerate the Syntheses of Well-Defined Polypeptides by N -Carboxyanhydride (NCA) Ring-Opening Polymerizations. *Macromolecules* **2013**, *46*, 4223–4226.
- (9) Fan, J.; Zou, J.; He, X.; Zhang, F.; Zhang, S.; Raymond, J. E.; Wooley, K. L. Tunable Mechano-Responsive Organogels by Ring-Opening Copolymerizations of N-Carboxyanhydrides. *Chem. Sci.* **2014**, *5*, 141–150.
- (10) Zhao, W.; Gnanou, Y.; Hadjichristidis, N. Fast and Living Ring-Opening Polymerization of  $\alpha$ -Amino Acid N-Carboxyanhydrides Triggered by an "Alliance" of Primary and Secondary Amines at Room Temperature. *Biomacromolecules* **2015**, *16*, 1352–1357.
- (11) Zhao, W.; Gnanou, Y.; Hadjichristidis, N. From Competition to Cooperation: A Highly Efficient Strategy towards Well-Defined (Co)Polypeptides. *Chem. Commun.* **2015**, *51*, 3663–3666.
- (12) Chen, C.; Fu, H.; Baumgartner, R.; Song, Z.; Lin, Y.; Cheng, J. Proximity-Induced Cooperative Polymerization in "Hinged" Helical Polypeptides. *J. Am. Chem. Soc.* **2019**, *141*, 8680–8683.
- (13) Song, Z.; Fu, H.; Baumgartner, R.; Zhu, L.; Shih, K. C.; Xia, Y.; Zheng, X.; Yin, L.; Chipot, C.; Lin, Y.; Cheng, J. Enzyme-Mimetic Self-Catalyzed Polymerization of Polypeptide Helices. *Nat. Commun.* **2019**, *10*, 5470–5477.
- (14) Wang, X.; Song, Z.; Tan, Z.; Zhu, L.; Xue, T.; Lv, S.; Fu, Z.; Zheng, X.; Ren, J.; Cheng, J. Facile Synthesis of Helical Multiblock Copolypeptides: Minimal Side Reactions with Accelerated Polymerization of N-Carboxyanhydrides. *ACS Macro Lett.* **2019**, *8*, 1517–1521.
- (15) Grazon, C.; Salas-Ambrosio, P.; Ibarboure, E.; Buol, A.; Garanger, E.; Grinstaff, M. W.; Lecommandoux, S.; Bonduelle, C. Aqueous Ring-Opening Polymerization-Induced Self-Assembly (RO-PISA) of N-Carboxyanhydrides. *Angew. Chem., Int. Ed.* **2020**, *132*, 632–636.
- (16) Wu, Y.; Chen, K.; Wu, X.; Liu, L.; Zhang, W.; Ding, Y.; Liu, S.; Zhou, M.; Shao, N.; Ji, Z.; Chen, J.; Zhu, M.; Liu, R. Superfast and Water-Insensitive Polymerization onα-Amino Acid N-Carboxyanhydrides to Prepare Polypeptides Using Tetraalkylammonium Carboxylate as the Initiator. *Angew. Chem., Int. Ed.* **2021**, *133*, 26267–26275.
- (17) Guo, L.; Zhang, D. Cyclic Poly(α-Peptoid)s and Their Block Copolymers from N-Heterocyclic Carbene-Mediated Ring-Opening Polymerizations of N-Substituted N-Carboxylanhydrides. *J. Am. Chem. Soc.* **2009**, *131*, 18072–18074.
- (18) Zhang, Y.; Liu, R.; Jin, H.; Song, W.; Augustine, R.; Kim, I. Straightforward Access to Linear and Cyclic Polypeptides. *Commun. Chem.* **2018**, *1*, 40–47.
- (19) Deming, T. J. Facile Synthesis of Block Copolypeptides of Defined Architecture. *Nature* **1997**, *390*, 386–389.
- (20) Raman, S. K.; Brulé, E.; Tschan, M. J.-L.; Thomas, C. M. Tandem Catalysis: A New Approach to Polypeptides and Cyclic Carbonates. *Chem. Commun.* **2014**, *50*, 13773–13776.
- (21) Deming, T. J. Transition Metal-Amine Initiators for Preparation of Well-Defined Poly(??-Benzyl L-Glutamate). *J. Am. Chem. Soc.* **1997**, 119, 2759–2760.
- (22) Cui, S.; Wang, X.; Li, Z.; Zhang, Q.; Wu, W.; Liu, J.; Wu, H.; Chen, C.; Guo, K. One-Pot Glovebox-Free Synthesis, Characterization, and Self-Assembly of Novel Amphiphilic Poly(Sarcosine-b-Caprolactone) Diblock Copolymers. *Macromol. Rapid Commun.* **2014**, 35, 1954–1959.
- (23) Cui, S.; Pan, X.; Gebru, H.; Wang, X.; Liu, J.; Liu, J.; Li, Z.; Guo, K. Amphiphilic Star-Shaped Poly(Sarcosine)-Block-Poly( $\varepsilon$ -Caprolactone) Diblock Copolymers: One-Pot Synthesis, Characterization, and Solution Properties. *J. Mater. Chem. B* **2017**, *5*, 679–690. (24) Guo, A. R.; Yang, W. X.; Yang, F.; Yu, R.; Wu, Y. X. Well-
- (24) Guo, A. R.; Yang, W. X.; Yang, F.; Yu, R.; Wu, Y. X. Well-Defined Poly(γ-benzyl-l-glutamate)-g-Polytetrahydrofuran: Synthesis,

- Characterization, and Properties. *Macromolecules* **2014**, 47, 5450–5461.
- (25) Deng, C.; Rong, G.; Tian, H.; Tang, Z.; Chen, X.; Jing, X. Synthesis and Characterization of Poly(Ethylene Glycol)-b-Poly (L-Lactide)-b-Poly(L-Glutamic Acid) Triblock Copolymer. *Polymer* **2005**, *46*, 653–659.
- (26) Planellas, M.; Puiggalí, J. Synthesis and Properties of Poly(L-Lactide)-b-Poly (L-Phenylalanine) Hybrid Copolymers. *Int. J. Mol. Sci.* **2014**, *15*, 13247–13266.
- (27) Price, D. J.; Khuphe, M.; Davies, R. P. W.; McLaughlan, J. R.; Ingram, N.; Thornton, P. D. Poly(Amino Acid)-Polyester Graft Copolymer Nanoparticles for the Acid-Mediated Release of Doxorubicin. *Chem. Commun.* **2017**, *53*, 8687–8690.
- (28) Duan, L. J.; Kim, M. J.; Jung, J. H.; Chung, D. J.; Kim, J. Synthesis of Poly(L,L-Lactic Acid-Co-Lysine) and Its Cell Compatibility Evaluation as Coating Material on Metal. *Macromol. Res.* **2010**, *18*, 806–811.
- (29) Birke, A.; Ling, J.; Barz, M. Polysarcosine-Containing Copolymers: Synthesis, Characterization, Self-Assembly, and Applications. *Prog. Polym. Sci.* **2018**, *81*, 163–208.
- (30) Dorresteijn, R.; Ragg, R.; Rago, G.; Billecke, N.; Bonn, M.; Parekh, S. H.; Battagliarin, G.; Peneva, K.; Wagner, M.; Klapper, M.; Müllen, K. Biocompatible Polylactide-Block-Polypeptide-Block-Polylactide Nanocarrier. *Biomacromolecules* **2013**, *14*, 1572–1577.
- (31) Sill, K. N.; Sullivan, B.; Carie, A.; Semple, J. E. Synthesis and Characterization of Micelle-Forming PEG-Poly(Amino Acid) Copolymers with Iron-Hydroxamate Cross-Linkable Blocks for Encapsulation and Release of Hydrophobic Drugs. *Biomacromolecules* **2017**, *18*, 1874–1884.
- (32) Caillol, S.; Lecommandoux, S.; Mingotaud, A. F.; Schappacher, M.; Soum, A.; Bryson, N.; Meyrueix, R. Synthesis and Self-Assembly Properties of Peptide-Polylactide Block Copolymers. *Macromolecules* **2003**, *36*, 1118–1124.
- (33) Peng, H.; Xiao, Y.; Mao, X.; Chen, L.; Crawford, R.; Whittaker, A. K. Amphiphilic Triblock Copolymers of Methoxy-Poly(Ethylene Glycol)-b-Poly(L-Lactide)-b-Poly(L-Lysine) for Enhancement of Osteoblast Attachment and Growth. *Biomacromolecules* **2009**, *10*, 95–104.
- (34) Tinajero-Díaz, E.; Martínez de Ilarduya, A.; Muñoz-Guerra, S. Synthesis and Properties of Diblock Copolymers of  $\omega$ -Pentadecalactone and  $\alpha$ -Amino Acids. *Eur. Polym. J.* **2019**, *116*, 169–179.
- (35) Gradišar, Š.; Žagar, E.; Pahovnik, D. Hybrid Block Copolymers of Polyesters/Polycarbonates and Polypeptides Synthesized via One-Pot Sequential Ring-Opening Polymerization. *Polym. Chem.* **2018**, *9*, 4764–4771.
- (36) Schmid, T. E.; Robert, C.; Richard, V.; Raman, S. K.; Guérineau, V.; Thomas, C. M. Aluminum-Catalyzed One-Pot Synthesis of Polyester-b-Polypeptide Block Copolymers by Ring-Opening Polymerization. *Macromol. Chem. Phys.* **2019**, 220, 1900040.
- (37) Teator, A. J.; Lastovickova, D. N.; Bielawski, C. W. Switchable Polymerization Catalysts. *Chem. Rev.* **2016**, *116*, 1969–1992.
- (38) Chen, C. Redox-Controlled Polymerization and Copolymerization. *ACS Catal.* **2018**, *8*, 5506–5514.
- (39) Broderick, E. M.; Guo, N.; Vogel, C. S.; Xu, C.; Sutter, J.; Miller, J. T.; Meyer, K.; Mehrkhodavandi, P.; Diaconescu, P. L. Redox Control of a Ring-Opening Polymerization Catalyst. *J. Am. Chem. Soc.* **2011**, *133*, 9278–9281.
- (40) Romain, C.; Zhu, Y.; Dingwall, P.; Paul, S.; Rzepa, H. S.; Buchard, A.; Williams, C. K. Chemoselective Polymerizations from Mixtures of Epoxide, Lactone, Anhydride, and Carbon Dioxide. *J. Am. Chem. Soc.* **2016**, *138*, 4120–4131.
- (41) Delle Chiaie, K. R.; Yablon, L. M.; Biernesser, A. B.; Michalowski, G. R.; Sudyn, A. W.; Byers, J. A. Redox-Triggered Crosslinking of a Degradable Polymer. *Polym. Chem.* **2016**, *7*, 4675–4681.
- (42) Lowe, M. Y.; Shu, S.; Quan, S. M.; Diaconescu, P. L. Investigation of Redox Switchable Titanium and Zirconium Catalysts for the Ring Opening Polymerization of Cyclic Esters and Epoxides. *Inorg. Chem. Front.* **2017**, *4*, 1798–1805.

- (43) Padilla-Vélez, O.; O'Connor, K. S.; Lapointe, A. M.; Macmillan, S. N.; Coates, G. W. Switchable Living Nickel(Ii)  $\alpha$ -Diimine Catalyst for Ethylene Polymerisation. *Chem. Commun.* **2019**, *55*, 7607–7610.
- (44) Zhao, Y.; Wang, Y.; Zhou, X.; Xue, Z.; Wang, X.; Xie, X.; Poli, R. Oxygen Triggered Switchable Polymerization for One-Pot Synthesis of CO2-Based Block Copolymers from Monomer Mixtures. *Angew. Chem., Int. Ed.* **2019**, *131*, 14449.
- (45) Yang, Q.; Wang, P.; Zhao, C.; Wang, W.; Yang, J.; Liu, Q. Light-Switchable Self-Healing Hydrogel Based on Host-Guest Macro-Crosslinking. *Macromol. Rapid Commun.* **2017**, 38, 1600741–1600747.
- (46) Tsai, C. C.; Payne, G. F.; Shen, J. Exploring PH-Responsive, Switchable Crosslinking Mechanisms for Programming Reconfigurable Hydrogels Based on Aminopolysaccharides. *Chem. Mater.* **2018**, 30, 8597–8605.
- (47) Paul, S.; Romain, C.; Shaw, J.; Williams, C. K. Sequence Selective Polymerization Catalysis: A New Route to ABA Block Copoly(Ester-b-Carbonate-b-Ester). *Macromolecules* **2015**, *48*, 6047–6056.
- (48) Darensbourg, D. J. Switchable Catalytic Processes Involving the Copolymerization of Epoxides and Carbon Dioxide for the Preparation of Block Polymers. *Inorg. Chem. Front.* **2017**, *4*, 412–419.
- (49) Li, M.; Zhang, P.; Chen, C. Light-Controlled Switchable Ring Opening Polymerization. *Macromolecules* **2019**, *52*, 5646–5651.
- (50) Nie, H.; Li, S.; Qian, S.; Han, Z.; Zhang, W. Switchable Reversible Addition—Fragmentation Chain Transfer (RAFT) Polymerization with the Assistance of Azobenzenes. *Angew. Chem., Int. Ed.* **2019**, *12*, 11571.
- (51) Biernesser, A. B.; Li, B.; Byers, J. A. Redox-Controlled Polymerization of Lactide Catalyzed by Bis(Imino)Pyridine Iron Bis(Alkoxide) Complexes. *J. Am. Chem. Soc.* **2013**, *135*, 16553–16560.
- (52) Gregson, C. K. A.; Gibson, V. C.; Long, N. J.; Marshall, E. L.; Oxford, P. J.; White, A. J. P. Redox Control within Single-Site Polymerization Catalysts. *J. Am. Chem. Soc.* **2006**, *128*, 7410–7411.
- (53) Lowe, M. Y.; Shu, S.; Quan, S. M.; Diaconescu, P. L. Investigation of Redox Switchable Titanium and Zirconium Catalysts for the Ring Opening Polymerization of Cyclic Esters and Epoxides. *Inorg. Chem. Front.* **2017**, *4*, 1798–1805.
- (54) Qi, M.; Dong, Q.; Wang, D.; Byers, J. A. Electrochemically Switchable Ring-Opening Polymerization of Lactide and Cyclohexene Oxide. J. Am. Chem. Soc. 2018, 140, 5686–5690.
- (55) Varnado, C. D.; Rosen, E. L.; Rosen, E. L.; Collins, M. S.; Lynch, V. M.; Bielawski, C. W. Synthesis and Study of Olefin Metathesis Catalysts Supported by Redox-Switchable Diaminocarbene[3]Ferrocenophanes. *Dalton Trans.* **2013**, 42, 13251–13264.
- (56) Lastovickova, D. N.; Shao, H.; Lu, G.; Liu, P.; Bielawski, C. W. A Ring-Opening Metathesis Polymerization Catalyst That Exhibits Redox-Switchable Monomer Selectivities. *Chem.—Eur. J.* **2017**, 23, 5994–6000.
- (57) Biernesser, A. B.; Delle Chiaie, K. R.; Curley, J. B.; Byers, J. A. Block Copolymerization of Lactide and an Epoxide Facilitated by a Redox Switchable Iron-Based Catalyst. *Angew. Chem., Int. Ed.* **2016**, 128, 5337–5340.
- (58) Qi, M. Electrochemically Switchable Polymerizations from Surface- Anchored Molecular Catalysts. *Chem. Sci.* **2021**, *12*, 9042.
- (59) Qi, M.; Zhang, H.; Dong, Q.; Li, J.; Musgrave, R. A.; Zhao, Y.; Dulock, N.; Wang, D.; Byers, J. A. Electrochemically Switchable Polymerization from Surface-Anchored Molecular Catalysts. *Chem. Sci.* **2021**, *12*, 9042–9052.
- (60) Wang, X.; Thevenon, A.; Brosmer, J. L.; Yu, I.; Khan, S. I.; Mehrkhodavandi, P.; Diaconescu, P. L. Redox Control of Group 4 Metal Ring-Opening Polymerization Activity toward l -Lactide and  $\varepsilon$ -Caprolactone. *J. Am. Chem. Soc.* **2014**, *136*, 11264–11267.
- (61) Delle Chiaie, K. R.; Biernesser, A. B.; Ortuño, M. A.; Dereli, B.; Iovan, D. A.; Wilding, M. J. T.; Li, B.; Cramer, C. J.; Byers, J. A. The Role of Ligand Redox Non-Innocence in Ring-Opening Polymer-

ization Reactions Catalysed by Bis(Imino)Pyridine Iron Alkoxide Complexes. *Dalton Trans.* **2017**, *46*, 12971–12980.

- (62) A light scattering detector was not available for absolute molecular weight measurements of pure polyamides.
- (63) Gradišar, Š.; Žagar, E.; Pahovnik, D. Ring-Opening Polymerization of N-Carboxyanhydrides Initiated by a Hydroxyl Group. *ACS Macro Lett.* **2017**, *6*, 637–640.
- (64) Goodman, M.; Arnon, U. The Mechanism of Strong-Base-Initiated Polymerization of N-Carboxyanhydrides. *J. Am. Chem. Soc.* **1964**, *86*, 3384–3390.
- (65) Wu, Y.; Zhang, D.; Ma, P.; Zhou, R.; Hua, L.; Liu, R. Lithium Hexamethyldisilazide Initiated Superfast Ring Opening Polymerization of Alpha-Amino Acid N-Carboxyanhydrides. *Nat. Commun.* **2018**, *9*, 5297–5310.
- (66) The mechanistic hypothesis presented in Scheme 3 is one that is consistent with all of the experimental information, but others may be possible.
- (67) Klinker, K.; Schäfer, O.; Huesmann, D.; Bauer, T.; Capelôa, L.; Braun, L.; Stergiou, N.; Schinnerer, M.; Dirisala, A.; Miyata, K.; Osada, K.; Cabral, H.; Kataoka, K.; Barz, M. Secondary-Structure-Driven Self-Assembly of Reactive Polypept(o)Ides: Controlling Size, Shape, and Function of Core Cross-Linked Nanostructures. *Angew. Chem., Int. Ed.* **2017**, *56*, 9608–9613.
- (68) Bauer, T. A.; Imschweiler, J.; Muhl, C.; Weber, B.; Barz, M. Secondary Structure-Driven Self-Assembly of Thiol-Reactive Polypept(o)Ides. *Biomacromolecules* **2021**, 22, 2171–2180.
- (69) Ortuño, M. A.; Dereli, B.; Chiaie, K. R. D.; Biernesser, A. B.; Qi, M.; Byers, J. A.; Cramer, C. J. The Role of Alkoxide Initiator, Spin State, and Oxidation State in Ring-Opening Polymerization of  $\epsilon$ -Caprolactone Catalyzed by Iron Bis(Imino)Pyridine Complexes. *Inorg. Chem.* **2018**, *57*, 2064–2071.
- (70) When BLG-NCA was used instead of Sar-NCA only homopolymers were observed. This outcome is believed to be due to deprotonation of the NH bond as was observed with other alkoxide initiators.
- (71) We have generated iron alkoxide initiators in situ using iron alkyl precatalysts before, see ref 51.
- (72) THF is polymerized by 4 in the presence of cyclohexene oxide.
- (73) A solvent and column suitable for obtaining molecular weight measurements of polysarcosine, poly(cyclohexene oxide), and the various copolymers was not found. Polysarcosine chromatographs were obtained using RI Detector in DMF with 0.01 M LiBr at 50 °C.

### **□** Recommended by ACS

#### **Compact Rotaxane Superbases**

Martin J. Power, David A. Leigh, et al.

APRIL 11, 2023

JOURNAL OF THE AMERICAN CHEMICAL SOCIETY

READ **C** 

## **Embedding Peptides into Synthetic Polymers: Radical Ring-Opening Copolymerization of Cyclic Peptides**

Federica Sbordone, Hendrik Frisch, et al.

MARCH 10, 2023

JOURNAL OF THE AMERICAN CHEMICAL SOCIETY

READ 🗹

#### Macrocyclic Allylic Sulfone as a Universal Comonomer in Organocatalyzed Photocontrolled Radical Copolymerization with Vinyl Monomers

Wenqi Wang, Jia Niu, et al.

JANUARY 18, 2023

MACROMOLECULES

READ 🗹

#### Protodemetalation of (Bipyridyl)Ni(II)—Aryl Complexes Shows Evidence for Five-, Six-, and Seven-Membered Cyclic Pathways

Paige E. Piszel, Daniel J. Weix, et al.

APRIL 07, 2023

JOURNAL OF THE AMERICAN CHEMICAL SOCIETY

READ 🗹

Get More Suggestions >